RSC Advances

PAPER

View Article Online
View Journal | View Issue

Cite this: *RSC Adv.*, 2021, **11**, 39680

Metabolome-based profiling of African baobab fruit (*Adansonia digitata* L.) using a multiplex approach of MS and NMR techniques in relation to its biological activity†

Mostafa H. Baky, ‡[a] Marwa T. Badawy,‡[b] Alaa F. Bakr,[c] Nesrine M. Hegazi, [d] Ahmed Abdellatif [b] and Mohamed A. Farag *[ef]

Adansonia digitata L. also known as African baobab is one of the most important fruit-producing trees, widely distributed in the African continent. Baobab fruits are known to possess potential health benefits and nutritional value. This study aimed to holistically dissect the metabolome of *A. digitata* fruits using a novel comparative protocol using three different analytical platforms. Ultra high performance liquid chromatography coupled to high-resolution tandem mass spectrometry (UHPLC-HRMS/MS), and headspace solid-phase microextraction/gas chromatography coupled to mass spectrometry (HS-SPME/GC-MS) were respectively employed for phytonutrients and aroma profiling, whereas GC-MS post silylation provided an overview of nutrients *i.e.*, sugars. UHPLC-HRMS/MS analysis allowed for the assignment of 77 metabolites, among which 50% are reported for the first time in the fruit. While GC-MS of silylated and aroma compounds led to the identification of 74 and 16 compounds, respectively. Finally, NMR-based metabolite fingerprinting permitted the quantification of the major metabolites for future standardization. In parallel, *in vivo* antidiabetic potential of the baobab fruit using a streptozotocin (STZ) induced diabetic rat model was assessed. Histopathological and immune-histochemical investigations revealed hepatoprotective and renoprotective effects of *A. digitata* fruit along with mitigation against diabetes complications. Moreover, the administration of *A. digitata* fruits (150 mg kg^{-1}) twice a week lowered fasting blood glucose levels.

Received 11th November 2021
Accepted 6th December 2021

DOI: 10.1039/d1ra08277a

rsc.li/rsc-advances

1. Introduction

African baobab (*Adansonia digitata* L.) belonging to the family Malvaceae is a large sub-tropical tree widely distributed in Southern, West, and East Africa.[1] Baobab is considered an extremely important edible fruit with myriad traditional uses and is widely consumed in African countries owing to its medicinal importance in the treatment of fever, diarrhea, and dysentery. Additionally, it is used as an immuno-stimulant, analgesic, antimalarial, and insect repellent.[1] Further, baobab fruit is recognized for its nutritional value and has been approved as a food ingredient in the European continent and the United States of America.[1,2]

In West Africa, the fruit pulp and seeds are consumed as food and as an ingredient in other food-based products such as sauces, porridges, and beverages.[3] Baobab fruit pulp is an essential source of vitamins, minerals, carbohydrates, amino acids, fatty acids, and sterols.[3] In addition, baobab is highly rich in vitamin C as it supplies 150–500 mg/100 g fruit so it is useful as a potent antioxidant and about 40 g of baobab pulp consumption daily provides 100% of the daily required vitamin C.[4] Baobab fruit is also rich in fibers, calcium, and vitamin B, and is low in proteins and fats.[5] The fresh fruit pulp is acidic in taste and consumed in African countries as a snack or as a refreshing juice by adding milk or water. Baobab edible fruits were reported to be enriched in various phytochemical compounds belonging to different chemical classes such as flavonoids, triterpenoids, steroids, vitamins, amino acids,

[a]*Pharmacognosy Department, Faculty of Pharmacy, Egyptian Russian University, Badr City, Cairo, 11829, Egypt. E-mail: dr_mostafa1984@yahoo.com; mostafa-hasan@eru.edu.eg; Tel: +01007906443*

[b]*Biology Department, School of Sciences & Engineering, The American University in Cairo, New Cairo 11835, Egypt*

[c]*Pathology Department, Faculty of Veterinary Medicine, Cairo University, Gamaa St., 12211 Giza, Egypt*

[d]*Phytochemistry and Plant Systematics Department, Division of Pharmaceutical Industries, National Research Centre, P. O. Box 12622, Cairo, Egypt*

[e]*Pharmacognosy Department, College of Pharmacy, Cairo University, Kasr El Aini St., P.B. 11562 Cairo, Egypt. E-mail: mohamed.farag@pharma.cu.edu.eg; Fax: +011-202-25320005; Tel: +011-202-2362245*

[f]*Chemistry Department, School of Sciences & Engineering, The American University in Cairo, New Cairo 11835, Egypt*

† Electronic supplementary information (ESI) available. See DOI: 10.1039/d1ra08277a

‡ Equally contributed to the work.

lipids, and carbohydrates.[6] Reported biological properties of baobab include anti-hyperglycemic,[7] analgesic and antipyretic, antibacterial, anti-inflammatory, antioxidant, and antiviral.[5]

Recently, modern analytical approaches especially metabolomics platforms have been used in the chemical analysis of food and spices.[8] Among analytical tools, UHPLC-HRMS/MS, GC/MS and NMR spectroscopy have been extensively adopted to characterize the metabolite diversity, *e.g.*, volatiles and non-volatiles in fruits and seeds.[9,10] Lastly, SPME is considered a convenient solvent-free method that requires minimal sample preparation for the enhancement of volatiles recovery from food samples.[11,12]

To the best of our knowledge, this is the first report on holistic metabolites profiling of *A. digitata* L., metabolites using 3 different analytical platforms *i.e.*, UHPLC-HRMS/MS, headspace SPME-GC/MS, GC/MS post silylation, and NMR simultaneously as a novel protocol for the determination of its quality characteristics. Additionally, molecular networks through the Global Natural Products Social Molecular Networking (GNPS) platform was exploited for the propagation of metabolites annotation from the UPLC-HRMS/MS dataset through the imaged structural similarities among the metabolites, with several novel metabolites reported for the first time. Moreover, the *in vivo* antidiabetic potential of *A. digitata* fruits was assessed in relation to the metabolites profile in streptozotocin (STZ)-induced diabetic animal model at multiple levels *i.e.*, histopathological examination and biochemical markers.

2. Materials and methods

2.1. Plant material and extract preparation

Adansonia digitata L. fruits (700 g) were purchased from a local market in Khartoum state, Sudan in January 2019. The air-dried powdered fruits (100 g) were extracted by soaking in 500 mL methanol for 48 h. The extract was then filtered and evaporated under reduced pressure at 40 °C and kept in a freezer at −10 °C for further investigation (6 g). A voucher specimen of the fruit material was deposited at the College of Pharmacy Herbarium, Cairo University, Cairo, Egypt.

2.2. Phytochemical investigation

2.2.1. Preparation of fruit extracts for UHPLC-MS analysis. The sample preparation method was performed as mentioned in ref. 13 with slight modifications. Briefly, 2 g of freeze-dried grounded fruits was homogenized with 5 mL 100% MeOH containing 10 μg mL^{-1} umbelliferone standard (Sigma-Aldrich, St. Louis, MO, US). The extract was then vortexed vigorously and centrifuged at 3000 g for 30 min to remove plant debris. For solid-phase extraction, 500 μL were aliquoted and loaded on a (500 mg) C18 cartridge, which was preconditioned with methanol and water. Samples were then eluted with 3 mL 70% MeOH and 3 mL 100% MeOH. The eluents were evaporated to dryness under a gentle nitrogen stream. The obtained dry residue was re-suspended in 500 μL methanol for further UHPLC-MS analysis.

2.2.2. UHPLC-HRMS/MS analysis. The UHPLC analysis was performed using an Acquity UHPLC System (Waters) equipped with a HSS T3 column (100 × 1.0 mm, particle size 1.8 μm; Waters). The analysis was carried out by applying the following binary gradient at a flow rate of 150 μL min^{-1}: 0–1 min, isocratic 95% A (water/formic acid, 99.9/0.1 [v/v]), 5% B (acetonitrile/formic acid, 99.9/0.1 [v/v]); 1–16 min, linear from 5 to 95% B; 16–18 min, isocratic 95% B; and 18–20 min, isocratic 5% B.[14] The injection volume was 3.1 μL (full loop injection). Eluted compounds were detected from *m*/*z* 90 to 1000 using a Micro-TOF-Q hybrid quadrupole time-of-flight mass spectrometer (Bruker Daltonics) equipped with an Apollo-II electrospray ion source in negative and positive (deviating values in brackets) ion modes using the following instrument settings previously reported.[15]

2.2.3. UPLC/MS metabolites data extraction and molecular networking. Bruker Daltonics Data Analysis 4.4 was used for UPLC/MS chromatograms inspection. While Metaboscape (Bruker Daltonics) 3.0 was used for data pre-processing using T-ReX 3D (Time aligned Region Complete eXtraction) algorithm for retention time alignment. Where isotopes, adducts, and fragments belonging to the same compound are automatically detected and combined into one feature. Detected features are displayed as a bucket table with their corresponding R_t, measured *m*/*z*, molecular weight, and detected fragments. The bucket table was created with an intensity threshold of $10e^4$ for both negative and positive ionization modes with a retention time range from 0 to 18 min and mass range from 120 to 1600 *m*/*z*.[16] For the molecular networking and metabolites annotation, the features list created by the Metaboscape was exported as an MGF file for both the positive and negative measurements. The negative and positive mode MGF files were uploaded independently to the GNPS online platform (https://gnps.ucsd.edu), where two molecular networks were created following the online workflow (GNPS 2.0). A molecular network was created with a cosine score above 0.65 and 0.7 for positive and negative modes, respectively, and the number of shared fragments was adjusted to 4. The networks were visualized using Cytoscape 3.5.1.[17]

2.2.4. SPME and chemicals. SPME fibers of stable flex coated with divinylbenzene/carboxen/polydimethylsiloxane (DVB/CAR/PDMS, 50/30_m) or PDMS (polydimethylsiloxane) were purchased from Supelco (Oakville, ON, Canada). All other chemicals, volatile standards, and sugars were purchased from Sigma Aldrich (St. Louis, MO, USA).

2.2.5. GC-MS analysis of silylated metabolites. Primary metabolite analysis was carried out as follows.[11,18] Briefly, 100 mg of finely powdered fruits were extracted with 5 mL 100% methanol with sonication for 30 min and frequent shaking, succeeded by centrifugation at 12 000 × *g* for 10 min to remove debris. 3 different samples for each *A. digitata* fruits accession were analyzed under the same conditions. Then, 100 μL of the methanol extract was aliquoted in screw-cap vials and left to evaporate under a nitrogen gas stream until complete dryness. For derivatization, 150 μL of *N*-methyl-*N*-(trimethylsilyl)-trifluoroacetamide (MSTFA) previously diluted 1 : 1% with

anhydrous pyridine was mixed with the dried methanol extract and incubated for 45 min at 60 °C prior to analysis using GC-MS. Separation of silylated derivatives was achieved on a Rtx-5MS (30 m length, 0.25 mm inner diameter, and 0.25 mm film). The protocol to validate silylation was adopted as previously reported.[18]

2.2.6. SPME-GC-MS volatile analysis. Dried, finely powdered fruits (20 mg) were placed in SPME screw-cap vials (1.5 mL) spiked with 10 μg (*Z*)-3-hexenyl acetate with fibers inserted manually above and placed in an oven kept at 50 °C for 30 min. HS-SPME analysis of the volatile compounds was performed as reported in ref. 18 with slight modifications. The fiber was subsequently withdrawn into the needle and then injected manually into the injection port of a gas chromatography-mass spectrometer (GC-MS). GC-MS analysis was adopted on an Agilent 5977B GC/MSD equipped with a DB-5 column (30 m × 0.25 mm i.d. × 0.25 m film thickness; Supelco) and coupled to a quadrupole mass spectrometer. The interface and the injector temperatures were both set at 220 °C. Volatile elution was carried out using the following gradient temperature program: oven was set at 40 °C for 3 min, then increased to 180 °C at a rate of 12 °C min^{-1}, kept at 180 °C for 5 min, finally increased at a rate of 40 °C min^{-1} to 240 °C and kept at this temperature for 5 min. Helium was utilized as a carrier gas with a total flow rate of 0.9 mL min^{-1}. For ensuring the complete elution of volatiles, SPME fiber was prepared for the next analysis by placing it in the injection port at 220 °C for 2 min. For assessment of biological replicates, three different samples for *A. digitata* fruits accession were analyzed under the same conditions.[10] Blank runs were made during sample analyses. The mass spectrometer was adjusted to EI mode at 70 eV with a scan range set at *m*/*z* 40–500.

2.2.7. GC/MS metabolites identification. Identification of volatile and non-volatile silylated components was performed by comparing their retention indices (RI) in relation to *n*-alkanes (C6–C20), mass matching to NIST, WILEY library database, and with standards if available. Peaks were first deconvoluted using AMDIS software (www.amdis.net (accessed on 28 November 2019))[18] before mass spectral matching.

2.3. Antidiabetic activity

2.3.1. Animals and induction of diabetes. All experiments were conducted following the NIH guidelines for animal care and use. Animal use protocol was approved by MSA University, Faculty of Biotechnology Animal Care and Use Committee (Courtesy of Dr Mona Saadeldin, MSA University). Study design and model intiation with the detailed methods were attached in the ESI (S-1).† Pancreatic tissue histological examination after animal termination confirmed diabetes mellitus.[19]

2.3.2. Histopathology and immunohistochemistry analysis. After 4 weeks of treatment, rats were sacrificed, and samples were collected (ESI, S-2 and S-3†). The liver, kidney, and pancreas tissues were treated as described by ref. 20. The scoring of liver and kidney damage was performed according to previous studies,[21] the grade of damage was obtained by adding the entire score of the types of histopathological lesions (4–5 field/rat/200×), as described in ESI Table S1.† Immunohistochemistry analysis of insulin was detected in the pancreatic sections according to the method described.[22]

2.3.3. Biochemical analysis. Glucose, creatinine, urea, uric acid, cholesterol, HDL, and TG were measured in mg dL^{-1}, whereas ALK, ALT, and AST were measured in IU L^{-1} (Spectrum Diagnostic, Germany) and detailed biochemical analysis was attached in the ESI (S-4).†

2.4. Statistical analysis

Data are presented as mean ± SD. One-way analysis of variance (ANOVA) followed by Tukey's comparison test was performed to compare parameters among groups. Data were analyzed by using R software (version 3.5.2) for biochemical analysis and parametric histological parameters. For non-parametric data (histological damage score), the statistics are presented as median ± SD using Kruskal–Wallis test, followed by Dunn's Multiple Comparison Test. A *P*-value of <0.05 was considered to be statically significant.

3. Results and discussion

Functional foods have had always played a pivotal role in developing countries as a potential source of alternative medicine. In Africa, several plants have been used traditionally for the management of diabetes mellitus. The present study aimed to characterize metabolites in baobab fruits *via* UHPLC/PDA/ESI-MS, and GC-MS techniques. While the quantification of the major metabolites was accomplished through NMR metabolite fingerprinting for future standardization. Further, the antidiabetic potential of *A. digitata* L. fruit extract in streptozotocin (STZ) induced diabetic rats model was investigated.

3.1. Phytochemical investigation

3.1.1. Secondary metabolites profiling of *A. digitata* L. fruit *via* UHPLC-HRMS/MS. In light of the reported biological properties of *A. digitata* L. fruits, a comprehensive investigation of its metabolites profile was achieved *via* reversed-phase UPLC/PDA/ESI-qTOF-MS using both positive and negative ionization modes targeting its secondary metabolites. Overlaid UPLC-MS base peak chromatograms (BPC) of *A. digitata* fruit extract in both ionization modes are shown in Fig. 1.

3.1.2. Molecular networking aided dereplication of *A. digitata* metabolites. Molecular networks assist the visual examination of mass spectrometry dataset, allowing for the propagation of metabolites annotation *via* the different metabolite classes, similarities among detected metabolites, and allowing for isomers detection. In this study, 2 molecular networks were generated for the positive and negative ionization modes dataset individually through GNPS 2 platform. The positive network had 287 nodes grouped into 26 clusters and 109 single nodes whereas the negative afforded a total of 161 nodes in 13 clusters and 47 isolated nodes (ESI Fig. S1†).

Metabolites dereplication was carried out based on their retention times, molecular formula, UV absorption maxima, and their fragmentation pattern in comparison to previously

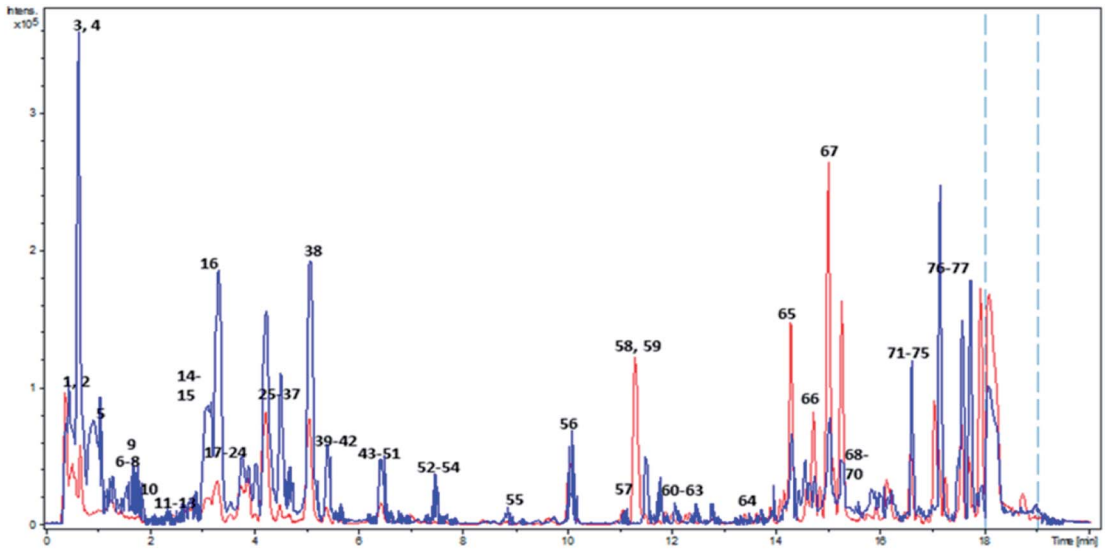

Fig. 1 Overlaid BPC of *Adansonia digitata* L. fruit crude extract in both ionization modes. Red and blue colors correspond to positive and negative ionization modes respectively. Peaks numbering follow that listed in Table 2.

reported data. 77 compounds were annotated belonging to different classes including organic acids, sugars, alcohols, phenolics, coumarins, and fatty acids. Almost 50% of the identified metabolites (40 compounds) are reported for the first time in *A. digitata* fruits (Table 1).

3.1.2.1. Organic acids. Citric acid and its isomer were detected in peaks 1 & 5 with $[M - H]^-$ at *m/z* 191.0198, $C_6H_8O_7$, and characteristic fragment at *m/z* 111. The negative molecular network (ESI Fig. S1,† cluster a) revealed a directly correlated ion at peak 6 $[M - H]^-$ 205.0354, $C_7H_{10}O_7$, with a mass difference of 14 Da (CH_2) and was annotated as citric acid methyl ester.[23]

Other organic acids included peak 2 with $[M - H]^-$ 133.0142, $C_4H_6O_5$ annotated as malic acid, and peak 13 with $[M - H]^-$ 175.0615, $C_7H_{12}O_5$.[24]

3.1.2.2. Saccharides and their derivatives. Cluster b of the negative spectral network (ESI Fig. S1†) compromised sugars and their derivatives from which peaks 3 & 4 corresponded to two disaccharides, where 3 had a molecular ion $[M - H]^-$ at *m/z* 341.1107, $C_{12}H_{22}O_{11}$ and was assigned as sucrose previously identified in *Adansonia* fruits.[25]

Butanediol-*O*-pentosyl-hexoside, peak 7 in the positive mode, showed a molecular ion at *m/z* 385.1699 $[M + H]^+$, $C_{15}H_{28}O_{11}$.[26] Similarly, peak 14 showed a molecular ion at *m/z* 369.1753 $[M + H]^+$, $C_{15}H_{28}O_{10}$ and a fragment at *m/z* 295 for the loss of C_4H_9O was assigned as butanol-pentosyl-hexoside.[27]

Additionally, the positive molecular network revealed the presence of 4 isomers of acylated hexoses; peaks 15, 25, 29 & 32 which shared a molecular ion at *m/z* 295.1018 $[M + H]^+$ and corresponded to the elemental composition of $C_{11}H_{18}O_9$.

3.1.2.3. Benzenoids & aromatics. Several phenolic metabolites were detected in both ionization modes and revealed themselves mostly as single nodes within both spectral networks. The first eluted at peak 8 was observed at $[M + H]^+$ at *m/z* 127.0393, $C_6H_6O_3$ with a fragment at *m/z* 109 for H_2O loss and was annotated as pyrogallol.[28] Following at peak 12, was dihydroxybenzaldehyde with $[M - H]^-$ at *m/z* 137.0243, $C_7H_6O_3$ and a characteristic fragment at *m/z* 109 for the cleavage of CO.[29] Lately eluted, peak 36 exhibited a molecular ion at *m/z* 461.1653 $[M - H]^-$ and elemental composition of $C_{20}H_{30}O_{12}$ and showing a daughter ion at *m/z* 149 $[M - H - 162 - 132]^-$ corresponding to the loss of a hexoside and pentoyl moieties.[30] Hence it was annotated as homovanillyl alcohol-*O*-pentosyl–*O*-hexoside. While peak 57 showed a molecular ion at *m/z* 149.0605 $[M - H]^-$, $C_9H_{10}O_2$ and a fragment at *m/z* 122 $[M - H - C_2H_2]^-$ was assigned as allylcatechol.[31]

Methoxybenzaldehyde, eluted in peak 60 with a molecular ion at *m/z* 137.0600 $[M + H]^+$, $C_8H_8O_2$ and fragment ion at *m/z* 122 and 109 for the consecutive cleavage of CH_3 and CO.[32] Similarly, peaks 61 & 62 with $[M - H]^+$ at *m/z* 133.0651, C_9H_8O, & 165.0907, $C_{10}H_{12}O_2$ and fragments at *m/z* 105 & 137 accounting for the loss of CO and were ascribed as cinnamaldehyde[33] and eugenol,[32] respectively.

The presence of benzoic acids in *A. digitata* fruits was previously reported[34] and was firstly observed in peak 9 assigned as vanillic acid from its molecular ion $[M - H]^-$ at *m/z* 167.0353, $C_8H_8O_4$ and fragment at *m/z* 123 $[M - H - 44]^-$ for the loss of CO_2.[35] Likewise, dihydroxybenzoic acid in peak 10 confirmed by its molecular ion at *m/z* 153.0193 $[M - H]^-$, $C_7H_6O_4$ and fragment at *m/z* 109 for the loss of CO_2.

3.1.2.4. Hydroxy cinnamates. Peaks 27 & 37 were annotated as hydroxyl cinnamic acid, *p*-coumaric acid isomers as concluded from their molecular ions at *m/z* 163.0401 $[M - H]^-$, 165.0544 $[M + H]^+$ and formula of $C_9H_8O_3$.[34] Quinic acid esters were detected in peaks 17 annotated as *O*-caffeoyl quinic acid ester (chlorogenic acid) and 35 & 40 as two isomers of *O*-feruloyl quinic acid. Peak 17 $[M - H]^-$at *m/z* 353.0891, $C_{16}H_{18}O_9$ and a base peak at *m/z* 191 suggestive for *O*-caffeoyl quinic acid ester (chlorogenic acid).[34] While peaks 35 & 40 showed same molecular ion at *m/z* 367.1024 $[M - H]^-$, $C_{17}H_{20}O_9$ and a base peak at *m/z* 191 confirming them to be isomers of *O*-feruloyl quinic acid esters.

Table 1 Metabolites identified in *A. digitata* fruits *via* UHPLC-MS/MS in 2 negative and positive ionization modes

Peak	Rt	Metabolite class	M − H	MS^2	M + H	MS^2	Chemical formula	Error (ppm)	Name	References
1	0.48	Organic acid	191.0198	129, 111			$C_6H_8O_7$	−0.14	Citric acid	67
2	0.48	Organic acid	133.0142	115			$C_4H_6O_5$	0.3	Malic acid	25
3	0.62	Saccharides	341.1091	179, 133	343.1234	163	$C_{12}H_{22}O_{11}$	0.06	Disaccharide (sucrose)	25
4	0.66	Saccharides	371.1196	325, 193			$C_{13}H_{24}O_{12}$	0.16	Unknown diasaccharide[a]	
5	0.75	Organic acid	191.0200	111			$C_6H_8O_7$	−1.87	Citric acid isomer	67
6	1.0	Organic acid	205.0354	111			$C_7H_{10}O_7$	−0.7	Citric acid methyl ester[a]	23
7	1.3	Saccharides			385.1699	163, 145	$C_{15}H_{28}O_{11}$	1.36	Butandiol pentoside hexoside[a]	26
8	1.39	Phenolic			127.0393	109	$C_6H_6O_3$	−4.05	Pyrogallol[a]	28
9	1.53	Benzoic acid	167.0353	123			$C_8H_8O_4$	2.05	Vanillic acid[a]	35
10	1.82	Benzoic acid	153.0193	109	155.0342	111	$C_7H_6O_4$	−2.02	Dihydroxy benzoic acid[a] (protocatechuic acid)	34
11	2.48	Nitrogenous compound			188.0701		$C_{11}H_9NO_2$	2.51	Unknown	
12	2.6	Benzenoids	137.0243	109			$C_7H_6O_3$	−2.6	Dihydroxybenzaldehyde[a]	29
13	2.84	Organic acid	175.0615	131, 157			$C_7H_{12}O_5$	−1.8	Hydroxyglutaric acid[a]	24
14	3.32	Saccharides derivatives			369.1753	295, 163, 145, 133, 115	$C_{15}H_{28}O_{10}$	0.38	Butanol hexopyranosyl-deoxypyranoside[a]	27
15	3.32	Saccharides derivatives			295.1012	163, 145, 133	$C_{11}H_{18}O_9$	2.55	Dihydroxy—methylenebutanoate-*O*-hexoside[a]	Tuliposide B[68]
16	3.39	Flavan-3-ol	289.0717	245, 203	291.0861	207, 139	$C_{15}H_{14}O_6$	2.42	Catechin/epicatechin	34 and 67
17	3.5	Cinnamic acid ester	353.0891	191			C16H18O9	−2.1	*O*-Caffeoyl quinic acid ester clorogenic acid	34
18	3.53	Nitrogenous compound	352.1034	191			$C_{16}H_{19}NO_8$	0.85	Unknown[a]	
19	3.72	Cinnamic acid ester	281.0660	193, 163, 145			$C_{13}H_{14}O_7$	4.39	*O*-feruloyl lactic acid ester[a]	36
20	3.79	Proanthocyanidin	577.1345	407, 289			$C_{30}H_{26}O_{12}$	−0.98	Procyanidn dimer isomer	Xx[34,67]
21	3.8	Cinnamic acid glycoside	327.1082	165, 147			$C_{15}H_{20}O_8$	2.8	Dihydrocoumaroyl *O*-hexoside (dihydromelilotoside)[a]	39
22	3.9	Proanthocyanidin	577.0346	407, 289	579.1472	409, 301, 291	$C_{30}H_{26}O_{12}$	4.25	Procyanidn dimer isomer I	34 and 67
23	3.91	Proanthocyanidin	865.1987			289	$C_{45}H_{38}O_{18}$	0.2	Procyanidin trimer isomer I	34 and 67
24	3.98	Cinnamic acids glycosides	341.0893	179 [M-H-162], 161			$C_{15}H_{18}O_9$	4.5	Caffeoyl–*O*-hexoside	40
25	4.03	Saccharides derivatives			295.1018	163, 145, 133	$C_{11}H_{18}O_9$	1.88	Dihydroxy–methylenebutanoate–*O*-hexoside isomer	68
26	4.1	Cinnamic acid glycosides	487.1457	193[M − H − 132-162]			$C_{21}H_{28}O_{13}$	−1.3	Feruloyl *O*-pentosyl hexoside[a]	41
27	4.23	Cinnamic acids			165.0544	119, 107	$C_9H_8O_3$	3.67	Coumaric acid	34
28	4.24	Flavan-3-ol	289.0716	245, 203	291.0860		$C_{15}H_{14}O_6$	−0.27	Catechin/epicatechin	34 and 67
29	4.33	Saccharides derivatives			295.1018	163, 145, 133	$C_{11}H_{18}O_9$	1.9	Dihydroxy-methylenebutanoic acid-*O*-hexoside	68
30	4.47	Cinnamic acid glycoside	325.0925	163			$C_{15}H_{18}O_8$	−0.29	Coumaroyl-*O*-hexoside[a]	41
31	4.52	Saccharides derivatives			383.1905	163, 145, 133, 155	$C_{16}H_{30}O_{10}$	1.7	Methylbutyl-*O*-pentosyl-hexoside[a]	68
32	4.52	Saccharides derivatives			295.1008	163, 145, 133	$C_{11}H_{18}O_9$	0.9	Dihydroxy-methylenebutanoic acid-*O*-hexoside	68
33	4.52	Proanthocyanidin	865.1992	577, 407, 289			$C_{45}H_{38}O_{18}$	1.03	Procyanidin trimer isomer II	Xx[34,67]
34	4.7	Proanthocyanidin	865.1994		867.1867	579, 289	$C_{45}H_{38}O_{18}$	0.77	Procyanidin trimer isomer	Xx[34,67]
35	4.73	Cinnamic acid ester selflooped	367.1024	191, 173, 133			$C_{17}H_{20}O_9$	−2.77	*O*-feruloyl quinic acid	Xx[67]
36	4.8	Phenolic	461.1653	149			$C_{20}H_{30}O_{12}$	4.5	Homovanillyl alcohol-*O*-pentosyl hexoside[a]	30
37	4.8	Cinnamic acid	163.0401	119			C9H8O3	−0.1	Coumaric acid isomer	34
38	5.02	Proanthocyanidin	1153.2595	865, 577, 289			$C_{60}H_{50}O_{24}$	−2.04	Procyanidin tetramer	34
39	5.1	Cinnamate			163.0391	135	$C_9H_8O_3$	−0.5	Unknown[a]	

Table 1 (*Contd.*)

Peak	Rt	Metabolite class	M − H	MS^2	M + H	MS^2	Chemical formula	Error (ppm)	Name	References
40	5.49	Cinnamic acid ester	367.1031	191, 173, 133			$C_{17}H_{20}O_9$	−0.52	*O*-feruloyl quinic acid isomer	67
41	5.59	Furanochromones			409.1111	247	$C_{19}H_{20}O_{10}$	4.37	Khellol-*O*-hexoside[a]	46
42	5.66	Flavonoid	609.1457	301			$C_{27}H_{30}O_{16}$	−0.65	Quercetin-*O*-deoxyhexosyl hexoside	67
43	6.2	Cinnamic acid glycoside	325.0916	163			$C_{15}H_{18}O_8$	−3.57	Coumaroyl-*O*-hexoside	40
44	6.27	Flavonoid	609.1467	301			$C_{27}H_{30}O_{16}$	1.04	Quercetin-*O*-deoxyhexosyl hexoside	67
45	6.43	Proanthocyanidin	577.1346	407, 289			$C_{30}H_{26}O_{12}$	−0.93	Procyanidn dimer isomer III	34 and 67
46	6.46	Flavonoid			449.1073	287	$C_{21}H_{20}O_{11}$	1.17	Kaempferol–*O*-hexoside	67
47	6.44	Flavonoid	593.1505	447, 285	595.1617	449, 287	$C_{27}H_{30}O_{15}$	1.04	Kaempferol–*O*-deoxyhexosyl hexoside[a]	43
48	6.47	Flavonoid			287.0543	217, 151	$C_{15}H_{10}O_6$	3.07	Kaempferol	67
49	6.52	Flavonoid	593.1505	447, 285			$C_{27}H_{30}O_{15}$	−2.46	Kaempferol–*O*-deoxyhexosyl hexoside isomer[a]	43
50	6.62	Cinnamic acid ester	293.0671	163, 145, 119			$C_{14}H_{14}O_7$	1.28	*O*-coumaroyl malic acid methyl ester[a]	37
51	6.88	Cinnamic acid glycosides	355.1022	193			$C_{16}H_{20}O_9$	−3.48	Feruloyl–*O*-hexoside	40
52	7.3	Cinnamic acid amide	326.1032	206, 163, 145			$C_{18}H_{17}NO_5$	−0.52	Coumaroyl–*N*-tyrosine[a]	38
53	7.5	Cinnamic acid	279.0870	163			$C_{14}H_{16}O_6$	1.6	Unknown[a]	
54	7.63	Flavonoid	447.09314	285			$C_{21}H_{20}O_{11}$	0.34	Kaempferol-*O*-hexoside	67
55	8.9	Megastigmane	405.2123	225			$C_{19}H_{34}O_9$	3.8	Megastigmane–*O*-hexoside[a]	69
56	10.1	Steroid	507.2582	345			$C_{27}H_{40}O_9$	0.9	Unknown	
57	11.2	Phenolic	149.0605	122			$C_9H_{10}O_2$	−1.68	Allyl catechol[a]	31
58	11.32	Furanochromones			261.0753	230	$C_{14}H_{12}O_5$	0.36	Khellin[a]	70
59	11.38	Furanochromones			231.0648	203, 216	$C_{13}H_{10}O_4$	1.35	Visnagin[a]	70
60	12.29	Phenolic			137.0600	122, 109	$C_8H_8O_2$	−2.2	Methoxy benzaldehyde	32
61	12.31	Phenolic			133.0651	105	C_9H_8O	2.94	Cinnamaldehyde	33
62	12.32	Phenolic			165.0907	137, 124	$C_{10}H_{12}O_2$	1.63	Eugenol	32
63	13.6	Cinnamic acid			207.1017	165, 150	$C_{12}H_{14}O_3$	−0.9	Unknown[a]	
64	13.72	Cinnamic acid			211.0961	193, 181, 165	$C_{11}H_{14}O_4$	1.55	Unknown[a]	
65	14.97	Coumarins			411.1410 [M + Na]	329, 245, 227, 199	$C_{21}H_{24}O_7$	0.81	Isovaleryl-acetyl khellactone (dihydrosamidin)[a]	47
66	14.98	Coumarins			329.1377	245, 227	$C_{19}H_{20}O_5$	1.9	Decursin[a]	51
67	15.1	Fatty acid	295.2274	277 ($-H_2O$), 233 ($-CO_2$)			$C_{18}H_{32}O_3$	1.3	Hydroxyoctadecadienoic acid[a]	71
68	15.1	Fatty acid	271.2278	253			$C_{16}H_{32}O_3$	1.2	Hydroxyhexadecanoic acid[a]	72
69	15.4	Fatty acid	269.2108	251		225	$C_{16}H_{30}O_3$	5.1	Oxohexadecanoic acid[a]	73
70	16.1	Fatty acid	295.2271	277 ($-H_2O$), 233 ($-CO_2$)			$C_{18}H_{32}O_3$	−3.1	Hydroxyoctadecadienoic acid[a]	74
71	16.1	Fatty acid	297.2423				$C_{18}H_{34}O_3$		Hydroxy-octadecanoic acid[a]	71
72	16.3	Fatty acid	311.2225	293 ($-H_2O$), 275 ($-H_2O$), 223			$C_{18}H_{32}O_4$	1.1	Dihydroxy-octadecadienoic acid[a]	74
73	16.6	Fatty acid	277.2171	259			$C_{18}H_{30}O_2$	1.8	Octadecatrienoic acid[a]	75
74	16.93	Fatty acid	355.3216	309			$C_{22}H_{44}O_3$	0.22	Hydroxydocosanoic acid[a]	72
75	17.1	Fatty acid	279.2331	261			$C_{18}H_{32}O_2$	−0.6	Octadecadienoic acid (linoleic acid)	75
76	17.5	Fatty acid	279.2331	261			$C_{18}H_{32}O_2$	−1.8	Octadecadienoic acid (linoleic acid)	75
77	17.6	Fatty acid	255.2333				$C_{16}H_{32}O_2$	−0.8	Hexadecanoic acid (palmitic acid)	76

[a] Metabolits detected for the first time from *Adansonia digitata* fruits.

Other identified cinnamate esters included peak 19 annotated as *O*-feruloyl lactic acid ester based on its $[M - H]^-$ at *m*/*z* 281.0660, $C_{13}H_{14}O_7$, and daughter ions at *m*/*z* 193 for the loss of lactic acid moiety ($C_3H_6O_3$).[36] Peak 50 with a $[M - H]^-$at *m*/*z* 293.0671 $[M - H]^-$, $C_{14}H_{14}O_7$ and fragment ions at *m*/*z* 163 $[M - H - 130]^-$ for the cleavage of $C_5H_6O_4$ (methyl malic acid) and *m*/

z 145 & 119 for dehydration and decarboxylation was annotated as *O*-*p*-coumaroyl malic acid methyl ester.[37] Whereas, coumaroyl tyrosine conjugate was detected in peak 52 with $[M - H]^-$at *m*/*z* 326.1032, and fragments at *m*/*z* 206 for tyrosine and subsequent fragments at *m*/*z* 163 and 145 for deamidation and dehydration.[38]

Cinnamic acid glycosides in peaks 21, 24, 30, 43, 51, all showed fragment ions $[M - H - 162]^-$ indicative of a hexoside moiety. Peak 21 was annotated as dihydrocoumaroyl *O*-hexoside (dihydromelilotoside) with $[M - H]^-$at *m*/*z* 327.1082, $C_{15}H_{20}O_8$,[39] and peak 24 as caffeoyl acid *O*-hexoside showing a molecular ion at *m*/*z* 341.0893 $[M - H]^-$, $C_{15}H_{18}O_9$.[40] Ferulic acid *O*-hexoside was observed in peak 51 with molecular ion at *m*/*z* 355.1022 $[M - H]^-$, $C_{16}H_{20}O_9$.[41] Additionally, feruloyl *O*-pentosyl hexoside peak 26 assignment was based on $[M - H]^-$ at *m*/*z* 487.1457, $C_{21}H_{28}O_{13}$ and fragment at *m*/*z* 193 corresponding to the loss of a hexoside and pentoside moieties.[41]

3.1.2.5. Proanthocyanidin and their monomers flavan-3-ol. Monomeric proanthocyanidins were detected in peaks 16 & 28 with molecular ions at *m*/*z* 289.0716 $[M - H]^-$, 291.0860 $[M + H]^+$, $C_{15}H_{14}O_6$, assigned as catechin/epicatechin.[34] In contrast, their dimeric procyanidins were observed in peaks 20, 22 & 45 with molecular ions at *m*/*z* 577.1346, $C_{30}H_{26}O_{12}$ with fragments at *m*/*z* 407, and 289 which are characteristic of type B proanthocyanidin previously reported in *A. digitata* fruits.[34] While, isomers of proanthocyanidin trimers were detected in peaks 23, 33 & 34 exhibiting molecular ions at *m*/*z* 865.1992, $C_{45}H_{38}O_{18}$ and distinctive fragments at *m*/*z* 577, 407, 289.[34] A procyanidin tetramer was recognized in peak 38 with a molecular ion at *m*/*z* 1153.2595 $[M - H]^-$, following the same fragmentation pattern as the dimers and trimers.[34] All detected proanthocyanidins were grouped in the negative molecular network as group c (ESI Fig. S1†) except for the tetramer which appeared as a self-looped node.

Proanthocyanidins are well known for their antidiabetic potential and to protect against diabetic complications to include oxidative stress, lipid peroxidation, diabetic encephalopathy, and retinopathy.[42]

3.1.2.6. Flavonoids. Aside from the flavan-3-ols, flavonols and their glycosides were depicted in peaks 42, 44, 46, 47, 48, 49 & 54. Quercetin-*O*-deoxyhexosyl hexoside isomers, 42 & 44 with a molecular ion at *m*/*z* 609.1457 $[M - H]^-$, $C_{27}H_{30}O_{16}$ showed the characteristic fragmentation for the loss of a hexoside and deoxyhexoside moieties to yield aglycone moiety at *m*/*z* 301.[34] Similarly, isomers of kaempferol-*O*-deoxyhexosyl hexoside were detected in peaks 47 & 49 with *m*/*z* 593.1505 $[M - H]^-$, $C_{27}H_{30}O_{15}$ and fragments at *m*/*z* 447 and 285.[43] While, peaks 46 & 54 were annotated as kaempferol-*O*-hexoside isomers at *m*/*z* 447.09314, $C_{21}H_{20}O_{11}$ and fragment at *m*/*z* 285. Several studies have affirmed the potential of dietary flavonoids in diabetes management through improving glucose metabolism and the lipid profile, thus protecting against diabetes and its aggravations.[44]

3.1.2.7. Furano- & pyrano-coumarins. Furanochromones were observed for the first time in peaks 41, 58 & 59 as proved from their molecular ions and fragmentation pattern detected solely in the positive ionization mode.[45]

Peak 41 detected in the positive ionization mode exhibited $[M + H]^+$ at *m*/*z* 409.1111, $C_{19}H_{20}O_{10}$ and a distinct fragment at *m*/*z* 247 for the loss of a hexoside moiety,[46] annotated as khellol-*O*-hexoside. While, peaks 58 & 59 with molecular ions at *m*/*z* 261.0753 $[M + H]^+$, $C_{14}H_{12}O_5$ and *m*/*z* 231.0648 $[M + H]^+$, $C_{13}H_{10}O_4$ were annotated as khellin and visnagin, respectively as concluded from their fragmentation pattern.

Likewise, pyranocoumarins were also detected for the first time in *A. digitata* fruits. An acylated derivative of the pyranocoumarin, khellactone was recognized at peak 65 as a Na adduct at *m*/*z* 411.1410 corresponding to $C_{21}H_{24}O_7$ as previously detected by.[47] Its MS^2 spectrum showed fragments at *m*/*z* 329 $[M + Na - C_2H_3O_2]^+$ for the cleavage of an acetic acid moiety, *m*/*z* 245 for the consecutive loss of an isovaleryl moiety (C_5H_8O) followed by *m*/*z* 227 and 199 for the elimination of H_2O and CO. Consequently, it was annotated as isovaleryl-acetyl khellactone.[47] *O*-Substituted esters of khellactone are reported to exhibit numerous biological activities *i.e.*, anti-obesity,[48] anti-HIV,[49] and anti-cancer[50] activities.

Similarly, peak 66 found in the positive ionization mode, with molecular ion at *m*/*z* 329.1377, $C_{19}H_{20}O_5$ was annotated as decursin following its fragmentation pattern with fragment ions at *m*/*z* 245 $[M + H - C_5H_8O]^+$.[51]

3.1.3. Primary metabolites profiling of *A. digitata* fruits *via* GC-MS post-silylation. To provide an overview of primary metabolites accounting for fruits' nutritional value, GC-MS analysis was employed post-silylation. A total of 74 peaks (Table 2 and Fig. 2) were annotated, including nitrogenous compounds, organic acids, sugars (mono- and disaccharides), sugar alcohols, and fatty acids, in addition to minor sterols and phenolics.

3.1.3.1. Sugars/sugar alcohols. Sugars, mostly monosaccharides represented the most dominant primary metabolite class at *ca.* 47% of total detected metabolites, comprising 25 different sugars. Glucose (peaks 40 and 41) was the main sugar (15%) detected in baobab fruit followed by arabinose (peak 38) and fructose (peak 37) detected at 6.5 and 5.2%, respectively. Such high level of glucose and other monosaccharides accounts for baobab fruits sweet taste. In contrast, major disaccharides in baobab were found to be melibiose (peak 50 and 52) and galactinol (peak 51) to amount for *ca*. 5% of the total sugars. Galactinol is one of the raffinose family oligosaccharides that was identified in baobab fruit, with potential antioxidant action.[52]

Sugar alcohols amounted for 13.2% of baobab fruit total metabolites detected using GC/MS. Mannitol (6.2%) and myo-inositol amounted for the major sugar alcohols in the fruit. Myo-inositol (peaks 56 and 57), the most abundant inositol isomer in cereals, and fruits, improves insulin sensitivity.[53] Consequently, baobab fruit could represent a potential functional food for diabetic patients based on these results.

3.1.3.2. Organic acids. Baobab fruit showed a considerable level of organic acids to account for the fruits acidic taste (12.5%) represented by malic acid (4.8%) and citric acid (2.5%). Malic acid is a common acid in unripe fruit, is used to enhance beverages flavor and to act as a food acidulant.[54]

Table 2 The relative percentage of silylated metabolites in *A. digitata* fruits analyzed *via* GC-MS, $n = 3$

No	Class	RT	KI	Name	Relative percentile ($n = 2$)
1	Nitrogenous compounds	8.203	1135.3	Hydroxylamine (3TMS)	0.32 ± 0.14
2		11.4365	1264.4	Urea (2TMS)	0.023 ± 0.01
3		13.7775	1355.4	Uracil (2TMS)	0.001 ± 0.0
4		18.5075	1545.7	4-Aminobutanoic acid (3TMS)	0.35 ± 0.07
5		25.5705	1864.6	*N*-Acetyl-galactosamine (TMS)	1.09 ± 0.46
6		35.3	2357.7	9-Octadecenamide (TMS)	2.55 ± 0.26
7		35.7485	2380.5	5-Methyluridine, (3TMS)	0.169 ± 0.12
8		37.4285	2466	(*Z*)-Docos-9-enenitrile (TMS)	2.369 ± 0.01
9		41.7965	2688.2	13-Docosenamide (TMS)	1.97 ± 0.37
Total nitrogenous compounds					**8.842**
10	Acids	11.588	1270.3	Benzoic acid (TMS)	0.76 ± 0.34
11		12.9275	1322.4	Maleic acid, (2TMS)	0.17 ± 0.16
12		13.5745	1347.5	Glyceric acid, (3TMS)	0.094 ± 0.06
13		13.905	1360.3	Itaconic acid, (2TMS)	0.19 ± 0.07
14		14.134	1369.2	Fumaric acid, (2TMS)	0.27 ± 0.21
15		14.403	1379.6	Nonanoic acid (TMS)	0.114 ± 0.04
16		15.5195	1423.7	Pentanedioic acid (2TMS)	0.0155 ± 0.01
17		17.5605	1506	Malic acid, (3TMS)	4.80 ± 2.5
18		21.061	1655.6	Tartaric acid (4TMS)	0.71 ± 0.22
19		23.601	1770.6	Aconitic acid (3TMS)	0.90 ± 0.088
20		24.961	1835	Shikimic acid (4TMS)	1.00 ± 0.23
21		25.067	1840.2	Citric acid (3TMS)	2.51 ± 3.55
22		25.818	1876.6	Quininic acid (5TMS)	0.994 ± 0.23
Total acids					**12.52**
23	Amino acids	11.775	1277.6	L-Serine (3TMS)	0.17 ± 0.02
24		12.677	1312.7	L-Threonine (2TMS)	0.054 ± 0.01
25		15.9605	1441.4	L-Aspartic acid (3TMS)	0.68 ± 0.23
26		18.2905	1536.6	Pyroglutamic acid (3TMS)	0.67 ± 0.04
27		18.642	1551.4	L-Glutamic acid (3TMS)	0.11 ± 0.05
Total amino acids					**1.69**
28	Sugars	15.212	1411.4	Ribonic acid (4TMS)	0.097 ± 0.01
29		19.2745	1577.9	Erythronic acid (4-TMS)	0.64 ± 0.15
30		20.551	1633.1	Ribofuranose, (4TMS)	0.12 ± 0.03
31		20.801	1644.1	Xylonic acid, (5TMS)	0.60 ± 0.03
32		21.6245	1680.4	Arabinose, (4TMS)	0.48 ± 0.19
33		22.9725	1741.7	Rhamnose (4TMS)	0.30 ± 0.12
34		23.2415	1754.1	Ribono-1,4-lactone (3TMS)	0.21 ± 0.01
35		24.4295	1809.3	Fructofuranoside (5TMS)	2.52 ± 1.85
36		25.9845	1884.7	Galactopyranose (5TMS)	0.40 ± 0.07
37		26.118	1891.2	Fructose (5TMS)	5.19 ± 0.83
38		26.398	1904.9	Arabinose (4TMS) isomer	6.47 ± 2.69
39		26.554	1912.9	Galactopyranose (5TMS) isomer	0.14 ± 0.03
40		26.730	1921.8	Glucose (5TMS)	12.16 ± 0.08
41		27.030	1937.1	Glucose (5TMS)	3.18 ± 4.5
42		27.161	1943.8	Glucono-1,4-lactone (4TMS)	0.14 ± 0.19
43		27.399	1955.9	Allose (5TMS)	0.43 ± 0.02
44		27.532	1962.6	Galactaric acid (6TMS)	1.43 ± 0.16
45		28.3115	2002.3	Talose (5TMS)	1.86 ± 0.49
46		28.566	2015.2	Gluconic acid (6TMS)	0.05 ± 0.06
47		37.7745	2483.6	Sucrose (8TMS)	0.66 ± 0.43
48		42.444	2721.1	Sedoheptulose anhydride (4TMS)	0.25 ± 0.18
49		43.6855	2784.3	Lactose (8TMS)	0.51 ± 0.38
50		44.253	2813.1	Melibiose (8TMS)	2.88 ± 0.15
51		44.4365	2822.5	Galactinol (9TMS)	4.07 ± 1.54
52		44.5525	2828.4	Melibiose (8TMS) isomer	2.22 ± 2.60
Total sugars					**47.00**
53	Sugar alcohol	17.834	1517.5	Threitol (4TMS)	0.11 ± 0.04
		18.017	1525.2	Threitol (4TMS) isomer 1	0.21 ± 0.08
54		21.624	1680.4	Threitol (4TMS) isomer 2	0.17 ± 0.23
55		27.262	1948.9	Mannitol (6TMS)	6.17 ± 8.39
56		29.185	2046.7	Myo-inositol (6TMS)	1.09 ± 1.55

Table 2 (*Contd.*)

No	Class	RT	KI	Name	Relative percentile (n = 2)
57		30.361	2106.5	Myo-inositol (6TMS) isomer	4.60 ± 0.62
58		36.0015	2393.4	Myo-inositol, (5TMS) phosphate	0.87 ± 0.25
Total sugar alcohols					**13.22**
59	Phenolics	18.6975	1553.7	Pyrogallol (3TMS)	0.032 ± 0.0
60		20.194	1617.3	Pyrogallol (3TMS) (isomer)	0.07 ± 0.07
61		42.7805	2738.2	Catechin (5TMS)	4.90 ± 0.06
Total phenolics					**5.0**
62	Fatty acids/glycerides	29.6455	2070.1	Palmitic acid (TMS)	0.65 ± 0.91
63		32.77	2229	Oleic acid (TMS)	0.92 ± 0.04
64		33.248	2253.4	Stearic acid (TMS)	0.45 ± 0.1
65		36.0975	2398.3	Oleamide (TMS)	1.06 ± 1.09
66		36.505	2419	Stearamide (TMS)	0.80 ± 0.34
67		38.8645	2539	Monopalmitin (2TMS)	1.24 ± 0.11
68		42.5505	2726.5	Lignoceric acid (TMS)	0.08 ± 0.05
Total fatty acids/glycerides					**5.2**
69	Steroids/terpenes	44.6665	2834.2	α-Tocopherol (TMS)	0.83 ± 0.22
70		48.153	3011.5	Campesterol (TMS)	0.25 ± 0.02
71		48.557	3032	Stigmasterol (TMS)	0.15 ± 0.03
72		49.603	3085.2	Stigmast-5-ene (TMS)	2.13 ± 0.22
Total steroids/terpenes					**3.36**
73	Inorganics	12.1065	1290.5	Phosphoric acid (3TMS)	2.94 ± 0.83
Total inorganics					**2.94**
74	Lactones			Dihydro-2(3*H*)-furanone (2TMS)	0.01 ± 0.02
Total lactones					**0.01**

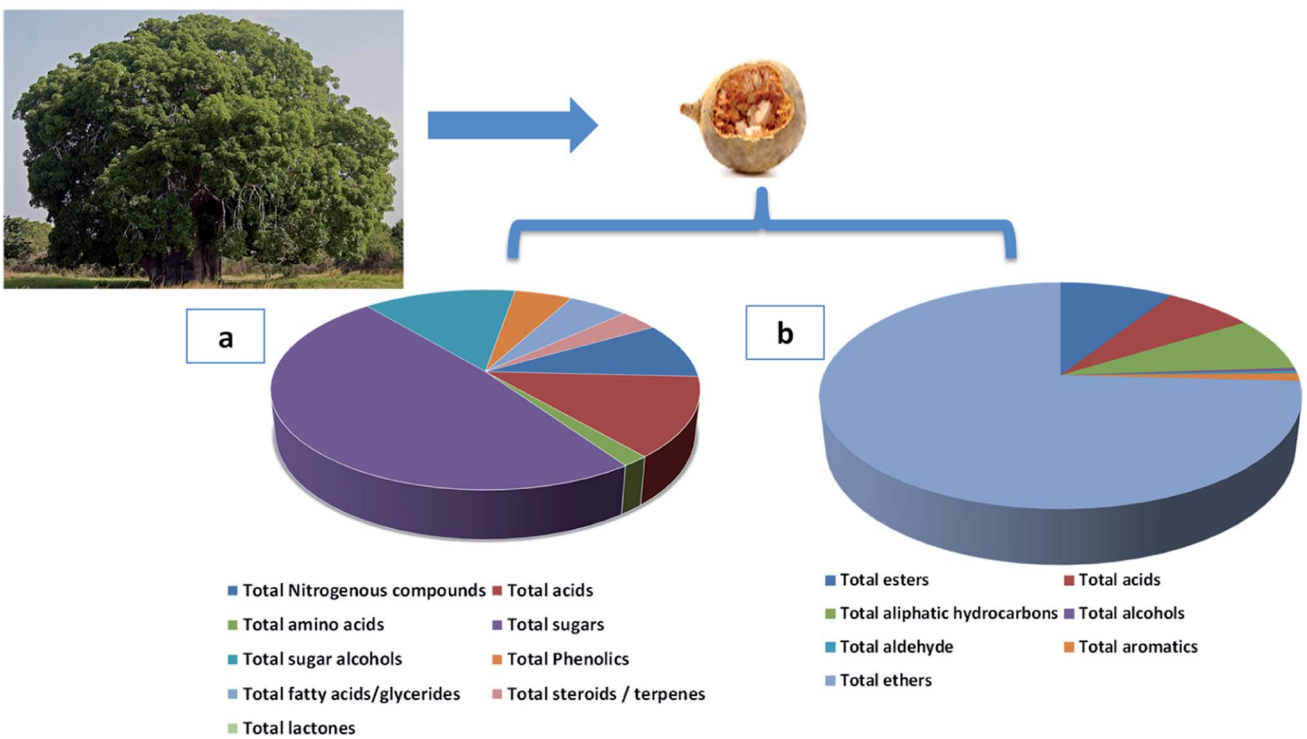

Fig. 2 *Adansonia digitata* tree and its fruit and pie charts of different metabolites classes. (a) The major non-volatile metabolites groups identified by GC-MS/MS post-silylation (b) the groups of identified aroma metabolites in *A. digitata* fruits using HS-SPME-GC-MS/MS.

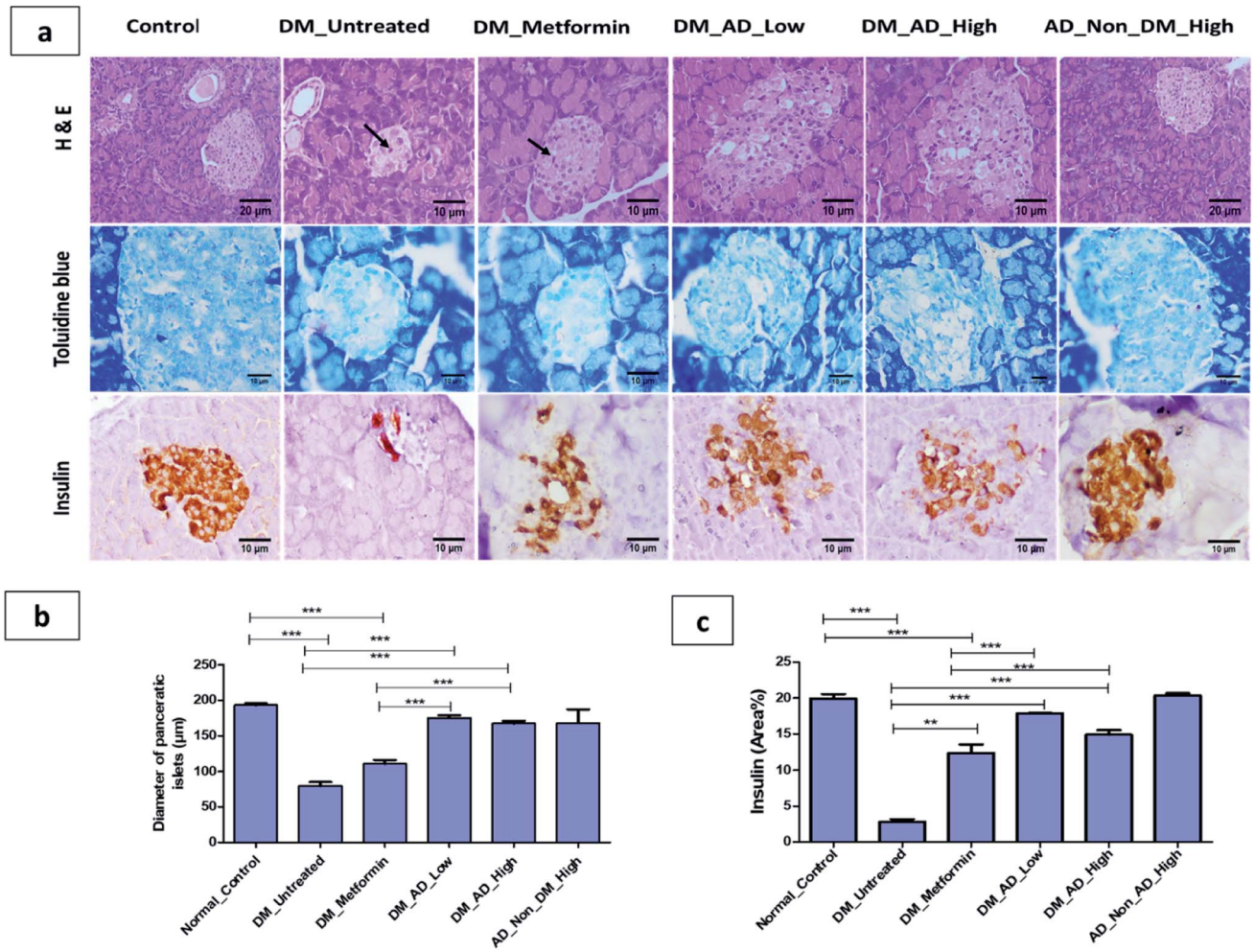

Fig. 3 (a)Photomicrographs of pancerase stained by hematoxylin and eosin, toluidine blue and insulin immunohistochemical staining. (b) The diameter of pancreatic islets (µm). (c) Immunohistochemical analysis for area% of insulin expression. Data expressed as mean ± SD (**P < 0.01, ***P < 0.001). Notable arrows on the figure indicate necrobiotic changes in ß-cells.

3.1.3.3. Nitrogenous compounds/amino acids. Nitrogenous compounds were detected in *A. digitata* fruit at 8.8% represented mostly by 9-octadecenamide (peak 6) and docos-9-enenitrile (peak 8) at 2.55 and 2.37%, respectively. *N*-Acetyl-D-galactosamine (peak 5), an amino sugar derivative of galactose was detected in baobab fruit which plays a role in mucin formation, aside for its effect on immune system and cancer.[55] The low amino acids level in baobab fruit (1.7%) suggests for its low pool in free amino acids, represented by pyroglutamic (peak 26), aspartic (peak 25), and glutamic (peak 27) acids.

3.1.3.4. Fatty acids/acyl esters/sterols. Fatty acids were detected in baobab fruit reaching 5.2% represented mostly by palmitic and oleic acids. Concerning fatty acyl esters, 1-monopalmitin (peak 67) was detected at 1.2%. Minor steroids were detected in baobab fruit to reach 3.36%, with stigmast-5-ene (peak 72, 2.13%) was found to be the dominant steroid.

3.1.3.5. Inorganic acids. Phosphoric acid (peak 73) was the only inorganic detected in *A. digitata* fruits at (2.9%). Phosphoric acid was reported to improve the antioxidant activity of tocopherols, aside from functioning as food preservative.[56]

3.1.3.6. Phenolics. Another considerable metabolite class detected in *A. digitata* fruits were phenolics detected at 5%. The major identified phenolics included catechin (peak 61), also detected using LC/MS. Catechin, a flavan-3-ol derivative common with antioxidant, antihyperlipidemic, and antidiabetic activities, and likely to account for fruit effects.[57]

3.1.4. Aroma analysis of *A. digitata* fruits using headspace SPME-GC-MS. *A. digitata* was subjected to volatile analysis likely to account for its organoleptic characters. HS-SPME led to the identification of 16 volatiles belonging to organic acids, alcohols, aldehydes, esters, ketones, aliphatic hydrocarbons, aromatics, and ethers (Table 3 and Fig. 2).

Ethers were detected as the major class in *A. digitata* fruit (74.5%), represented mostly by isoeugenol (peak 18). Isoeugenol is a common flavoring agent used as a food preservative owing to its antimicrobial activity.[58] The relative amounts of both organic acids and esters in *A. digitata* were at *ca.* 9.1 and 7.1% of total detected aroma compounds, respectively. Hexadecanoic acid methyl ester (peak 3, 8.1%) was the most abundant ester in *A. digitata* fruit to mediate for its antimicrobial properties.[59]

In contrast, alcohols were detected at trace levels of 0.5% represented by linalool (peak 14) a monoterpene alcohol used as flavoring and antibacterial agent.[60] Aliphatic hydrocarbons accounted for 7.8% of the volatile composition in baobab fruit. Major forms included 1,3-butadiene, 2,3-dimethyl (peak 6), and 2,4-hexadiene (peak 7) at 3.2 and 1.8%, respectively. Aromatic compounds were also detected at a low level at 1.13% of the total volatiles represented by *o*-cymene (peak 16) and *p*-cymene (peak 17).

3.1.5. NMR-based metabolites fingerprinting of *A. digitata* fruits. NMR fingerprinting was employed for the analysis of *A. digitata* fruits. Peaks assignment was established on the previously reported chemical shifts in literature. Further, 2D-NMR experiments were employed including ^{1}H–^{1}H-COSY, ^{1}H–^{13}C HSQC (heteronuclear single quantum coherence spectroscopy), and HMBC (heteronuclear multiple bond correlation). 15 Metabolites were identified and listed with their respective chemical shifts in ESI Table 1.† The illustrative ^{1}H-NMR spectrum of *A. digitata* fruit extract is shown in ESI Fig. 2.†

Typically, ^{1}H-NMR spectrum of *A. digitata* fruits compromised two main regions, a low field region (δ 0.5–5.5 ppm) with more abundant signals of the primary metabolites (ESI Fig. 2a†), and a high field region of much lower abundance corresponding to secondary metabolites to account more for fruits health effects (ESI Fig. 2b†). Primary metabolites identified included fatty acids (**N1** & **N2**), amino acids (**N3–N8**), organic acids (**N9** & **N10**), and sugars (**N11–N13**). While secondary metabolites belonged to flavonoids (**N14–N15**), ESI Table S1.†

The first recognized metabolites in spectrum belonged to ω-6 fatty acids (**N1**) as evident from the broad signal at δ 0.87–0.91 ppm for the terminal methyl, δ 2.77 ppm for the allylic methylene and δ 5.36 for the olefinic protons.[13] A fatty acid ester (**N2**) was recognized from the upfield shifts of H-2 and H-3 at δ 2.26 and 1.53 ppm, respectively. Several amino acids were detected including (**N5**) leucine (δ 0.96 ppm, d, 5.4), (**N6**) alanine (δ 1.41 ppm, d, 7.2), and (**N8**) proline (δ 4.17 ppm, dd, 2.4, 7.2). Further, downfield region revealed the presence of aromatic amino acid *i.e.*,(**N7**) phenylalanine *via* its characteristic signals at δ 7.55 ppm (d, 1.8), δ 7.57 ppm (d, 2.4), and δ 7.58 ppm (d, 2.4).

The presence of other nitrogenous compounds *i.e.*, γ-aminobutyric acid (**N3**) was also evident from its signals at δ 1.973 ppm (m), 2.209 ppm (t, 7.2), and δ 2.72 ppm along with choline (**N4**) through the signal at δ 3.202 ppm (s). Besides the presence of organic acids were evident from signals ascribed to (**N9**) citric acid detected at δ 2.540 ppm (d, 15.6) and δ 2.567 ppm (d, 15.6), and (**N10**) malic acid with its signal at δ 4.091 ppm (dd, 12, 6). Citric and malic acids were detected also in GC-MS which indicate the efficiency of identification process, Table 2.

Sugars abundance observed from GC/MS Table 2, was also confirmed using ^{1}H-NMR spectrum, and in agreement with previous reports.[25] Sugars were assigned based on their characteristic anomeric signals at δ 4.401 ppm (d, 7.8) for β-glucose (**N11**), δ 5.033 ppm (d, 3.6) for α-glucose (**N12**), and δ 5.319 ppm (d, 3.6) for sucrose (**N13**).

Comparably, the aromatic region revealed much less abundant signals, mostly for flavonoids. As previously described, catechin and its conjugates (**N11**), were the major flavonoids assigned from signals at δ 5.841 ppm (d, 2.4), δ 5.86 ppm (d, 2.4) for H-6 & H-8, and characteristic multiplet at δ 3.965 ppm for H-

Table 3 The relative percentage of volatile constituents in *A. digitata* fruits analyzed using SPME–GC-MS, $n = 2$

No	Class	RT	KI	Name	Relative percentile
1	Ester	2.095	398	Acetic acid, methyl ester	0.45 ± 0.0
2		11.8654	1468	Terpinene 4-acetate	0.57 ± 0.0
3		16.1491	1916	Hexadecanoic acid methyl ester	8.05 ± 0.0
Total esters					**9.07**
4	Acids	2.3652	430	Acetic acid	6.80 ± 0.0
5		8.9189	1166	Octanoic acid	0.34 ± 0.0
Total acids					**7.14**
6	Aliphatic hydrocarbon	5.3152	784	1,3-Butadiene, 2,3-dimethyl	3.17 ± 0.0
7		7.1919	1007	2,4-Hexadiene	1.81 ± 0.0
8		9.283	1200	Dodecane	0.57 ± 0.0
9		11.163	1399	Tetradecane	0.68 ± 0.0
10		12.0777	1489	Pentadecane	0.79 ± 0.0
11		13.2017	1598	Hexadecane	0.79 ± 0.0
Total aliphatic hydrocarbons					**7.82**
12	Alcohol	8.2609	1106	β-Linalool	0.45 ± 0.0
Total alcohols					**0.45**
13	Aldehyde	8.304	1110	Nonanal	0.34 ± 0.0
Total aldehyde					**0.34**
14	Aromatic	8.5455	1132	*o*-Cymene	0.03 ± 0.0
15		12.0261	1484	*p*-Cymene	1.10 ± 0.0
Total aromatics					**1.13**
16	Ether	10.8708	1368	Isoeugenol	74.49 ± 0.0
Total ethers					**74.49**

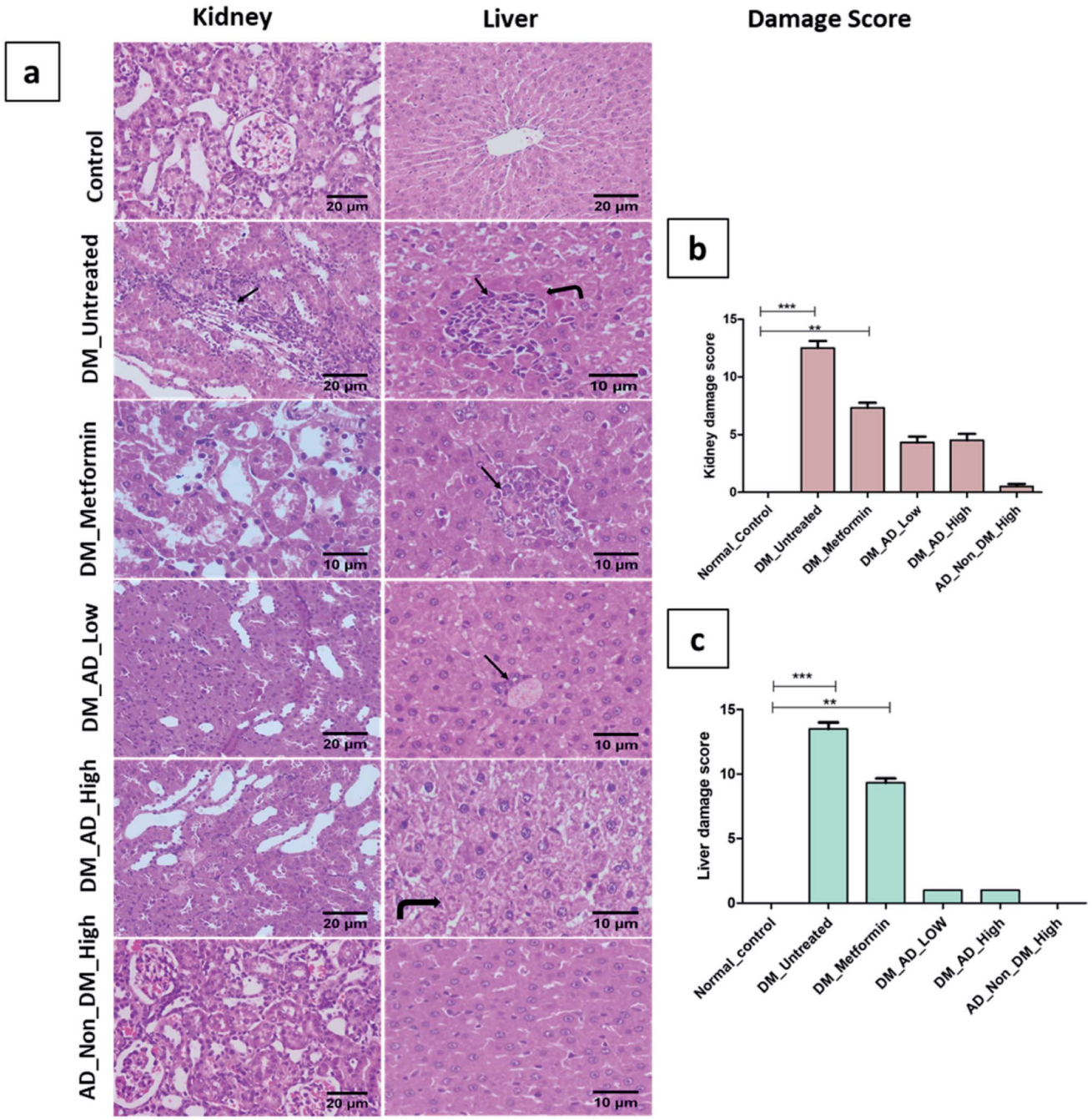

Fig. 4 (a) Photomicrographs of kidney and liver sections stained by (H&E). (b and c): histological damage score in kidney and liver tissues respectively. Data presented as median ± SD. $^{**}P < 0.01$, $^{***}P < 0.001$. Remarkable features are indicated on the figure as follows: inflammatory cell infiltration (arrow), coagulative necrosis (curved arrow).

3. Quercetin, a common flavonol *in planta* was also detected based on signals at δ 6.924 ppm (d, 2.4, H-6), δ 6.936 ppm (d, 2.4, H-8), and δ 7.148 ppm (d, 2.4). The enrichment of flavonoids is likely to account for fruits reported antioxidant and antidiabetic effects.[61]

3.1.6. Quantification of major metabolites detected *via* ^{1}H-NMR. ^{1}H-NMR was employed for the quantification of major primary and secondary metabolites in the *A. digitata* fruits for future standardization purposes (ESI Table S2†). Recently, NMR was successfully used for the quantification of metabolites with no standards required as in case of LC/MS.[62,63] Total sugars in *A. digitata* fruits were detected and quantified at 58.9 μg mg^{-1} with sucrose as the predominant sugar at 40.04 μg mg^{-1}, contributing to fruit sweetness. Another class to account for the taste were organic acids with a content of 5.5 μg mg^{-1}, mainly as malic acid (3.4 μg mg^{-1} dry powder) and citric acid (2.1 μg mg^{-1}

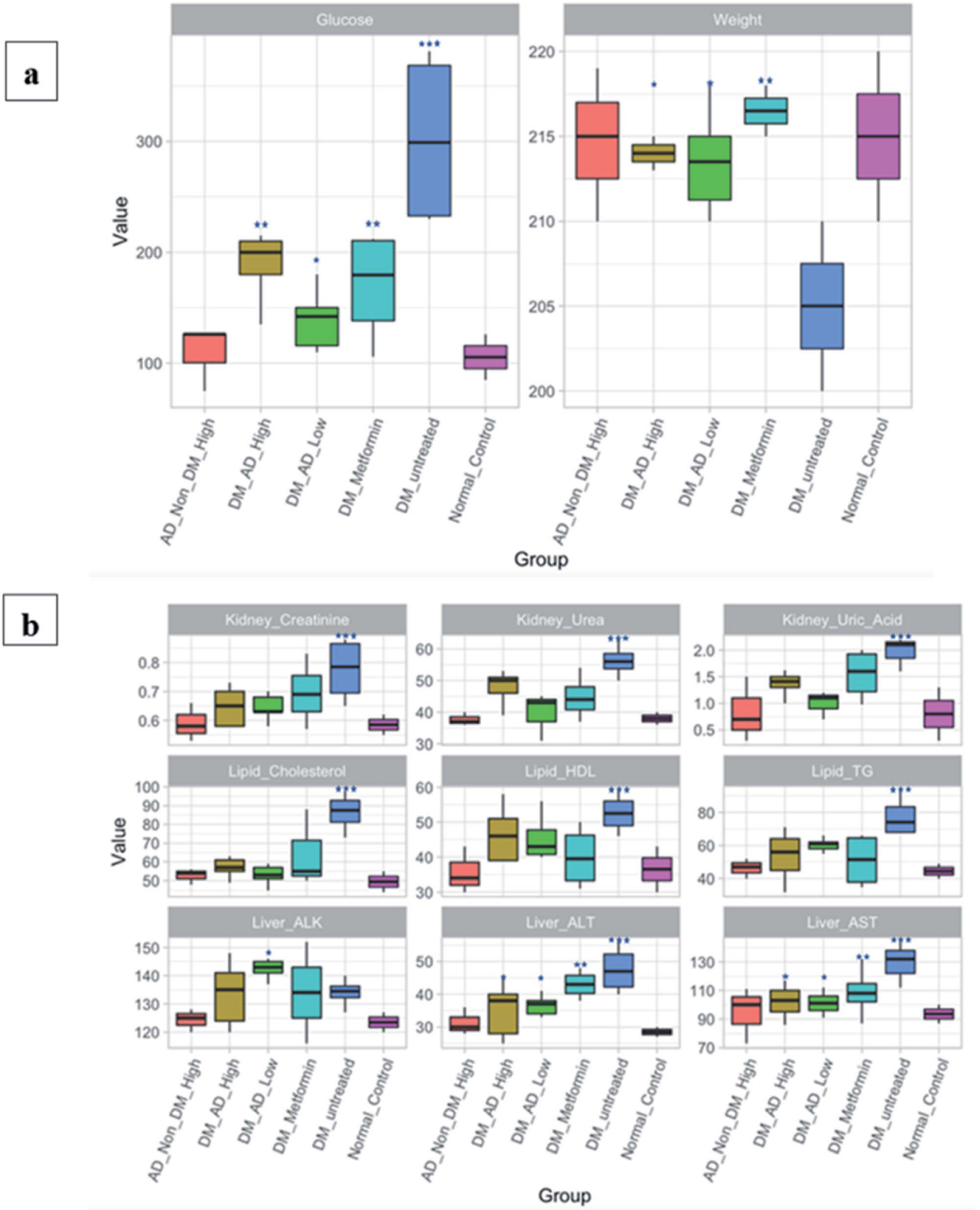

Fig. 5 (a) Fasting blood glucose (FBG) and body weight of rats. (b) Biochemical analyses of the lipid profile, liver, and kidney functions. The groups are normal healthy rats (Normal_Control), diabetic rats without any treatment (DM_Untreated), diabetic rats administrated metformin orally (DM_Metformin), diabetic rats i.p. injection with a low dose, which is 150 mg kg^{-1}, of *A. digitata* L. (DM_AD_Low), diabetic rats i.p. injection with high dose, which is 300 mg kg^{-1}, of *A. digitata* L. (DM_AD_High), and healthy rats i.p. injection with high dose of *A. digitata* L. (AD_Non_DM_High). Figure generated with R software version 3.5.2. Data expressed as mean ± SD (**$P < 0.01$, ***$P < 0.001$). The *Y*-axis is representing the values of each measured parameter; glucose, creatinine, urea, uric acid, cholesterol, HDL, and TG are measured in mg dL^{-1}, whereas ALK, ALT, and AST are measured in IU L^{-1}. Body weight is measured in grams.

dry powder). *A. digitata* fruits showed high choline level at 4.1 μg mg^{-1} dry powder adding to its nutritional value, being recognized as an essential nutrient for the body function.[64] In addition, flavonoids were detected and quantified in *A. digitata* fruits at 3.97 μg mg^{-1} dry powder and quercetin was detected as the major flavonoid. The abundance of flavonoids in the fruit add to its biological value as a potent antioxidant and antidiabetic phytochemicals.

3.2. Antidiabetic activity

A. digitata fruits' antidiabetic and its effect on tissues histopathology and different biochemical parameters related to diabetes were investigated *in vivo*.

3.2.1. Histopathological and immunohistochemistry analysis. Diabetes mellitus is often associated with pancreatic tissue damage, necrosis and microvascular vacuolization of the liver and nephropathy.[65] Histopathological examination of the pancreas, kidney, and liver tissues showed no significant difference between diabetic rats treated with a low or high dose of *A. digitata* (Fig. 3a and b). The elevated expression of insulin in ß-cells depicted in (Fig. 3c) was observed in both diabetic groups treated with 150 mg kg^{-1} and 300 mg kg^{-1} compared to the control group and metformin-treated group. These results are in accordance with the hypoglycemic effect of *A. digitata* through the enhancement of insulin production by ß cells, as previously reported.[66]

Similarly, vacuolar degeneration, necrobiotic changes, and interstitial nephritis were observed in diabetic untreated and metformin-treated groups. Treatment of diabetic rats with either low or high doses of *A. digitata* upgraded the histological structure of the kidney to normal (Fig. 4a), while the scoring description of kidney damage is depicted in (Fig. 4b).

In the same context, administration of *A. digitata* at both low and high doses improved the histological structure of the liver tissue of diabetic rats. Rats receiving 150 mg kg^{-1} of *A. digitata* showed restoration of cellular structure with minimal infiltration of inflammatory cells (Fig. 4a). The normal structure was observed in the group treated with only a high dose of *A. digitata* extract (Fig. 4a).

3.2.2. Biochemical assays. Administration of both metformin and *A. digitata* fruit at a high dose (300 mg kg^{-1}) sustained the blood glucose levels when compared to diabetic rats ($P < 0.01$). Unexpectedly, the lower dose treatment of the *A. digitata* fruit (150 mg kg^{-1}) recorded better results compared to the higher dose (Fig. 5a). Additionally, the ALT, AST, and lipid profile markers in significantly increased in the untreated diabetic group as illustrated in Fig. 5a. Contrariwise, the diabetic group treated with *A. digitata* L. at both doses showed a diminution in the ALT, AST ($P < 0.05$), triglycerides, and HDL ($P < 0.05$) compared to other groups. Moreover, cholesterol level was considerably reduced with *A. digitata* L. fruit extract at a dose of 300 mg kg^{-1}, and a more profound reduction was observed at the dose of 150 mg kg^{-1} ($P < 0.01$). Likewise, regarding the renal markers, *A. digitata* L. treated groups with both 150 mg kg^{-1} and 300 mg kg^{-1} showed a significant reduction in the creatinine level compared to the diabetic group ($P < 0.05$).

4. Conclusion

In the present study, holistic metabolites profiling of *A. digitata* fruits was achieved *via* different metabolomics platforms. UPLC-MS/MS permitted for the dereplication of 77 compounds belonging to different classes, including organic acids, sugars, alcohols, phenolics, coumarins, and fatty acids. Almost 50% of the identified metabolites (40 compounds) are reported for the first time in *A. digitata* fruits. GC/MS investigation for both non-volatile and volatile metabolites revealed the identification of 74 non-volatile and 16 volatile compounds. Lastly, identification and quantification of the major metabolites was possible through the employment of 1D-NMR and 2D-NMR spectroscopy. While the investigated fruit is from one origin, same metabolomics platform can be used to assess fruits from other origins for comparative analysis. Simultaneously, the antidiabetic potential of *A. digitata* fruits extract was also investigated revealing potent activity owing to the abundance of bioactive phytochemicals in the fruits. Histopathological and immunohistochemical studies demonstrated the hepatoprotective and renoprotective effects of *A. digitata* fruits in STZ induced diabetic rats. Biochemical assays revealed its capacity to lower the fasting glucose, lipid profile, hepatic and renal markers. Further investigations are required for deeper pharmacological, physiological, and biochemical insights and the determination of the optimum therapeutic dose.

Funding

The work was funded by AUC financial support.

Author contributions

Mostafa H. Baky: data curation; writing – review. Marwa T. Badawy: data curation, writing – review. Alaa F. Bakr: writing – review. Nesrine M. Hegazi: data curation; writing – review. Ahmed Abdellatif: writing – review. Mohamed A. Farag: supervision, writing – review & editing.

Conflicts of interest

There is no conflict of interest.

Acknowledgements

Dr Mohamed Farag would like to thank the Alexander Von Humboldt foundation, Germany for funding. The authors would like to acknowledge the contribution of Ms. Eman A. Khalil in facilitating some procedures in histopathology investigation.

References

1 G. Kamatou, I. Vermaak and A. Viljoen, *S. Afr. J. Bot.*, 2011, 77, 908–919.

2 A. Lamien-Meda, C. E. Lamien, M. M. Compaoré, R. N. Meda, M. Kiendrebeogo, B. Zeba, J. F. Millogo and O. G. Nacoulma, *Molecules*, 2008, **13**, 581–594.
3 F. Chadare, A. Linnemann, J. Hounhouigan, M. Nout and M. Van Boekel, *Crit. Rev. Food Sci. Nutr.*, 2008, **49**, 254–274.
4 J. Scheuring, M. Sidibé and M. Frigg, *Sight and Life Newsletter*, 1999, **1**, 21–24.
5 C. Buchmann, S. Prehsler, A. Hartl and C. R. Vogl, *Ecol. Food Nutr.*, 2010, **49**, 145–172.
6 Y. Shukla, S. Dubey, S. Jain and S. Kumar, *J. Med. Aromat. Plant Sci.*, 2001, **23**, 429–434.
7 M. Y. Gwarzo and H. u. Y. Bako, *Int. J. Anim. Vet. Adv.*, 2013, **5**, 108–113.
8 M. A. Farag, A. R. Khattab, A. A. Maamoun, M. Kropf and A. G. Heiss, *Food Res. Int.*, 2019, **115**, 379–392.
9 S. M. Afifi, A. El-Mahis, A. G. Heiss and M. A. Farag, *ACS Omega*, 2021, **6**, 5775–5785.
10 M. A. Farag, S. M. Afifi, D. M. Rasheed and A. R. Khattab, *J. Food Compos. Anal.*, 2021, 104073.
11 M. A. Farag, D. Fathi, S. Shamma, M. S. A. Shawkat, S. M. Shalabi, H. R. El Seedi and S. M. Afifi, *LWT*, 2021, **142**, 111046.
12 M. H. Baky, M. A. Farag and D. M. Rasheed, *ACS omega*, 2020, **5**, 31370–31380.
13 M. A. Farag, A. Otify, A. Porzel, C. G. Michel, A. Elsayed and L. A. Wessjohann, *Anal. Bioanal. Chem.*, 2016, **408**, 3125–3143.
14 M. Farag, E. Mahrous, T. Lübken, A. Porzel and L. Wessjohann, *Metabolomics*, 2013, **10**, 21–32.
15 M. A. Farag, A. Otify, A. Porzel, C. G. Michel, A. Elsayed and L. A. Wessjohann, *Anal. Bioanal. Chem.*, 2016, **408**, 3125–3143.
16 L. Olmo-García, K. Wendt, N. Kessler, A. Bajoub, A. Fernández-Gutiérrez, C. Baessmann and A. Carrasco-Pancorbo, *Eur. J. Lipid Sci. Technol.*, 2019, **121**, 1800336.
17 M. E. Smoot, K. Ono, J. Ruscheinski, P. L. Wang and T. Ideker, *Bioinformatics*, 2011, **27**, 431–432.
18 M. A. Farag, A. R. Khattab, S. Shamma and S. M. Afifi, *Foods*, 2021, **10**, 728.
19 N. A. Qinna and A. A. Badwan, *Drug Des., Dev. Ther.*, 2015, **9**, 2515–2525.
20 D. Ahmed, V. Kumar, A. Verma, G. S. Shukla and M. Sharma, *Springerplus*, 2015, **4**, 1–17.
21 R. Klopfleisch, *BMC Vet. Res.*, 2013, **9**(1), 1–15.
22 G. B. Ha, E. J. Park, J. E. Shin and H. Y. Shon, *PloS one*, 2014, **9**(7), 1–12.
23 L. Makila, O. Laaksonen, A.-L. Alanne, M. Kortesniemi, H. Kallio and B. Yang, *J. Agric. Food Chem.*, 2016, **64**, 4584–4598.
24 P. Lorenz, J. Conrad, J. Bertrams, M. Berger, S. Duckstein, U. Meyer and F. C. Stintzing, *Phytochem. Anal.*, 2012, **23**, 60–71.
25 A. J. T. Sokeng, A. P. Sobolev, A. Di Lorenzo, J. Xiao, L. Mannina, D. Capitani and M. Daglia, *Food Chem.*, 2019, **272**, 93–108.
26 H. Sun, J. Liu, A. Zhang, Y. Zhang, X. Meng, Y. Han, Y. Zhang and X. Wang, *J. Sep. Sci.*, 2016, **39**, 496–502.
27 E. Fujimatu, T. Ishikawa and J. Kitajima, *Phytochemistry*, 2003, **63**, 609–616.
28 H. Tohma, İ. Gülçin, E. Bursal, A. C. Gören, S. H. Alwasel and E. Köksal, *J. Food Meas. Charact.*, 2017, **11**, 556–566.
29 M. Lutter, A. C. Clark, P. D. Prenzler and G. R. Scollary, *Food Chem.*, 2007, **105**, 968–975.
30 Y. Zhang, L.-J. Yang, K. Jiang, C.-H. Tan, J.-J. Tan, P.-M. Yang and D.-Y. Zhu, *Carbohydr. Res.*, 2012, **361**, 114–119.
31 N. F. Abdullah and R. Mohamad Hussain, *J. Liq. Chromatogr. Relat. Technol.*, 2015, **38**, 289–293.
32 O. Razanamaro, E. Rasoamanana, B. Rakouth, J. R. Randriamalala, E. Rabakonadrianina, A. Clément-Vidal, J.-M. L. P. Tsy, C. Menut and P. Danthu, *Biochem. Syst. Ecol.*, 2015, **60**, 238–248.
33 J. A. Seukep, A. G. Fankam, D. E. Djeussi, I. K. Voukeng, S. B. Tankeo, J. A. Noumdem, A. H. Kuete and V. Kuete, *Springerplus*, 2013, **2**, 363.
34 B. B. Ismail, Y. Pu, M. Guo, X. Ma and D. Liu, *Food Chem.*, 2019, **277**, 279–288.
35 J. Gruz, O. Novák and M. Strnad, *Food Chem.*, 2008, **111**, 789–794.
36 S. Wu, A. E. Wilson, L. Chang and L. Tian, *Molecules*, 2019, **24**, 3814.
37 M. K. Lee, H. Y. Jeon, K. Y. Lee, S. H. Kim, C. J. Ma, S. H. Sung, H.-S. Lee, M. J. Park and Y. C. Kim, *Planta Med.*, 2007, **73**, 782–786.
38 M. N. Clifford and S. Knight, *Food Chem.*, 2004, **87**, 457–463.
39 L. Yang, N. Nakamura, M. Hattori, Z. Wang, S. A. Bligh and L. Xu, *Rapid Commun. Mass Spectrom.*, 2007, **21**, 1833–1840.
40 X.-N. Li, J. Sun, H. Shi, L. L. Yu, C. D. Ridge, E. P. Mazzola, C. Okunji, M. M. Iwu, T. K. Michel and P. Chen, *Food Res. Int.*, 2017, **99**, 755–761.
41 I. M. Abu-Reidah, D. Arráez-Román, A. Segura-Carretero and A. Fernández-Gutiérrez, *Food Res. Int.*, 2013, **51**, 354–362.
42 A. Rauf, M. Imran, T. Abu-Izneid, S. Patel, X. Pan, S. Naz, A. S. Silva, F. Saeed and H. A. R. Suleria, *Biomed. Pharmacother.*, 2019, **116**, 108999.
43 F. Ferreres, S. Magalhães, A. Gil-Izquierdo, P. Valentão, A. R. Cabrita, A. J. Fonseca and P. B. Andrade, *Food Chem.*, 2017, **214**, 678–685.
44 R. Vinayagam and B. Xu, *Nutr. Metab.*, 2015, **12**, 1–20.
45 M. Ganzera, S. Sturm and H. Stuppner, *Chromatographia*, 1997, **46**, 197–203.
46 R. Schuster, *Chromatographia*, 1980, **13**, 379–385.
47 D. N. Olennikov, I. A. Fedorov, N. I. Kashchenko, N. K. Chirikova and C. Vennos, *Molecules*, 2019, **24**, 2286.
48 N. Taira, R. N. Nugara, M. Inafuku, K. Takara, T. Ogi, T. Ichiba, H. Iwasaki, T. Okabe and H. Oku, *J. Funct. Foods*, 2017, **29**, 19–28.
49 L. Xie, Y. Takeuchi, L. M. Cosentino and K.-H. Lee, *J. Med. Chem.*, 1999, **42**, 2662–2672.
50 J. Y.-C. Wu, W.-F. Fong, J.-X. Zhang, C.-H. Leung, H.-L. Kwong, M.-S. Yang, D. Li and H.-Y. Cheung, *Eur. J. Pharmacol.*, 2003, **473**, 9–17.

51 H. J. Lee, H. J. Lee, E. O. Lee, J. H. Lee, K. S. Lee, K. H. Kim, S.-H. Kim and J. Lü, *Am. J. Chin. Med.*, 2009, **37**, 127–142.
52 A. Nishizawa, Y. Yabuta and S. Shigeoka, *Plant Physiol.*, 2008, **147**, 1251–1263.
53 M. L. Croze and C. O. Soulage, *Biochimie*, 2013, **95**, 1811–1827.
54 C. Pereira, L. Barros, A. M. Carvalho and I. C. Ferreira, *Food Anal. Methods*, 2013, **6**, 1337–1344.
55 L. Wells, in *Handbook of Glycomics*, Elsevier, 2010, pp. 45–57.
56 A. Saba, O. Benini and A. Cupisti, *Clinical Aspects of Natural and Added Phosphorus in Foods*, 2017, pp. 133–141.
57 T. Chanadiri, T. Sanikidze, M. Esaishvili, I. Chkhikvishvili and I. Datunashvili, *Georgian Med. News*, 2005, 61–63.
58 T. Koeduka, E. Fridman, D. R. Gang, D. G. Vassão, B. L. Jackson, C. M. Kish, I. Orlova, S. M. Spassova, N. G. Lewis and J. P. Noel, *Proc. Natl. Acad. Sci.*, 2006, **103**, 10128–10133.
59 M. T. Shaaban, M. F. Ghaly and S. M. Fahmi, *J. Basic Microbiol.*, 2021, **61**, 557–568.
60 M. Y. Issa, E. Mohsen, I. Y. Younis, E. S. Nofal and M. A. Farag, *Ind. Crops Prod.*, 2020, **144**, 112002.
61 R. G. C. Barros, U. C. Pereira, J. K. S. Andrade, C. S. de Oliveira, S. V. Vasconcelos and N. Narain, *Food Res. Int.*, 2020, **136**, 109614.
62 A. M. Otify, A. M. El-Sayed, C. G. Michel and M. A. Farag, *Metabolomics*, 2019, **15**, 119.
63 M. A. Farag, M. G. Sharaf El-Din, M. A. Selim, A. I. Owis, S. F. Abouzid, A. Porzel, L. A. Wessjohann and A. Otify, *Molecules*, 2021, **26**, 761.
64 T. C. Wallace, J. K. Blusztajn, M. A. Caudill, K. C. Klatt, E. Natker, S. H. Zeisel and K. M. Zelman, *Nutr. Today*, 2018, **53**, 240.
65 Y. Jaiswal, P. Tatke, S. Gabhe and A. Vaidya, *J. Tradit. Complement. Med.*, 2017, **7**, 421–427.
66 M. Y. Gwarzo, *Int. J. Anim. Vet. Adv.*, 2013, **5**, 108–113.
67 A. Braca, C. Sinisgalli, M. De Leo, B. Muscatello, P. L. Cioni, L. Milella, A. Ostuni, S. Giani and R. Sanogo, *Molecules*, 2018, **23**, 3104.
68 I. M. Abu-Reidah, D. Arráez-Román, M. Al-Nuri, I. Warad and A. Segura-Carretero, *Food Chem.*, 2019, **279**, 128–143.
69 K. Singh, B. K. Dubey, A. C. Tripathi, A. P. Singh and S. K. Saraf, *Nat. Prod. Res.*, 2014, **28**, 1313–1317.
70 P. Vanachayangkul, V. Butterweck and R. F. Frye, *J. Chromatogr. B*, 2009, **877**, 653–656.
71 A. Napolitano, A. Cerulli, C. Pizza and S. Piacente, *Food Chem.*, 2018, **269**, 125–135.
72 K. Feussner and I. Feussner, in *High-Throughput Metabolomics*, Springer, 2019, pp. 167–185.
73 K.-H. Nam, H. J. Kim, I.-S. Pack, H. J. Kim, Y. S. Chung, S. Y. Kim and C.-G. Kim, *Appl. Biol. Chem.*, 2019, **62**, 15.
74 Y. Liang, G. Y. Yan, J. L. Wu, X. Zong, Z. Liu, H. Zhou, L. Liu and N. Li, *Phytochem. Anal.*, 2018, **29**, 398–405.
75 M. A. Osman, *Plant Foods Hum. Nutr.*, 2004, **59**, 29–33.
76 G. Razafimamonjison, J. M. Leong Pock Tsy, M. Randriamiarinarivo, P. Ramanoelina, J. Rasoarahona, F. Fawbush and P. Danthu, *Chem. Biodiversity*, 2017, **14**, e1600441.